INTERNATIONAL SOCIETY FOR SOIL MECHANICS AND GEOTECHNICAL ENGINEERING

Numerical modelling of under-reamed scaled-down piles by water jet driving

Cesar Alberto Ruver[1#]

[1]*Federal University of Rio Grande do Sul, Civil Engineer Department, Osvaldo Aranha Avenue, 99, Porto Alegre, Brazil*
[#]*cesar@ufrgs.br*

ABSTRACT

Water jet pile driving technique has been shown to be viable for driving precast piles in highly resistant soil layers. However, the use of this technique drastically reduces the pile load capacity. On the other hand, the use of under-reamed precast piles improves the vertical load capacity. The objective of the present paper is to show the efficiency of the use of under-ream, through the numerical modelling of load tests carried out in laboratory scaled-down models. For numerical modelling, finite element method (FEM) was used. Through numerical analysis, it was possible to identify the distribution of stresses and strains at the toe, shaft, and under-reams. With that it was possible to identify and check the contribution of these in the total vertical compressive load capacity. It was possible to verify that the under-reams contribute to the vertical load capacity varying from 47% to 57% depending on the configuration, number, and distribution of the under-reams along the pile. Thus, increasing the final vertical load capacity, if compared to piles without under-ream (uniform shaft). Numerical modelling proved to be a fundamental tool, which made it possible to show the mechanisms involved in the action of under-ream in increasing the vertical load capacity of piles.

Keywords: precast under-reamed pile; numerical modelling of pile; water jet pile driving.

1. Introduction

The most common methodology to install precast piles in the soil is by driving with an impact hammer. Commonly used single-acting hammer by free fall (gravity effect). The Brazilian foundation standard, NBR 6122 (ABNT, 2019), recommends minimum weights. For example, for precast piles, hammers with a minimum weight of 40 kN are recommended for workloads between 0.7 and 1.3 MN, and in addition to a minimum weight of 75% of the pile weight. The standard also refers to the maximum limits of compressive and tensile stresses of driving systems, considering the resistance of the concrete. In this sense, if the hammer energy is not enough to break the resistance of soils, the specified depth will not be reached or there may be structural damage to the piles (breaking, warping, crushing, etc.) if too high potential energy is used. In these cases, the water jet driving technique can be used. But studies indicate (scaled-down models and field tests) that the use of water jet compromises the soil resistance around the piles, and thus, reduces the load capacity, both in compression and in traction, whether in sandy or clayey soils (Tsinker, 1988; Gunaratne et al., 1999; Mezzomo, 2009; Ruver et al., 2014; Passini, 2015; Moriyasu et al., 2016a, 2016b). Mezzomo (2009) and Passini (2015) observed that the relative density reaches a loose condition (approximately, $D_r = 30\%$) after using water jet, regardless of the initial relative density of the sand ($D_r = 50\%$ - medium and 90% - dense). Ruver et al. (2014) found a loss of load capacity between 53% and 90% in scaled-down models of concrete piles driven in fine sand,

compared to the same models driven by conventional percussion. The authors found that the highest load capacity losses occurred for higher jet flow rates. Passini (2015) found that the executive procedures (driving method) and the initial condition of the sand are some of the constraints that commanded the tensile load capacity of the tests performed. Ruver and Jong (2019), through a parametric study by numerical simulation, found that the initial density of the sand influences the load capacity of the piles driven by water jet, although the final compactness of the sand is the same around the pile.

To increase the load capacity of piles, regardless of the type of execution (precast or moulded in situ), some devices can be used. An example is the use of reamed sections or bulbs, which can be located at the toe or along the shaft of a pile. The most traditional cases are the belled shaft pile and the franki pile, which are made up of uniform shaft elements with the widening of the toe (Das and Sivakugan, 2018; ABNT, 2019). Several authors have studied the effects on the load capacity of reamed sections along the shaft and toe (single and multi-under-reamed pile), which are conducted in a scaled-down or true size model, varying the quantity, position and shape of the reams (Mohan et al., 1969; Yabuuchi and Hrayama, 1993; Lee, 2007; Hirai et al., 2008; Honda et al., 2011; Choi et al., 2013; Qian et al., 2013; Christopher and Goponath, 2015; George and Hari, 2015; Shetty et al., 2015; Zarrabi and Eslami, 2016; Moayedi and Mosallanezhad, 2017; Vali et al., 2017; Zhang et al, 2018; Majumder and Chakraborty, 2022; Ziyara and Albusoda, 2022). According to the authors, the insertion of reams considerably improves the load capacity of the piles, when compared to piles with continuous shaft

(without under-ream). The study carried out by Ruver (2013) shows the efficiency of a precast concrete pile model with three reams driven by water jet in sand, which presented more than twice the load capacity, compared to the same uniform pile (without under-ream).

To better understand the behaviour and the contribution of the reams, several authors have been performing numerical simulations (Lee, 2007; Honda et al., 2011; George and Hari, 2015; Harris and Madabhushi, 2015; Moayedi and Mosallanezhad, 2017; Vali et al., 2017; Jong, 2019; Ruver and Jong, 2019; Ruver et al., 2019; Majumder and Chakraborty, 2022; Ziyara and Albusoda, 2022). In this context, studies by Jong (2019) and Ruver et al. (2019), who performed numerical and parametric simulations to find an under-reamed pile that enhances the load capacity, varying the number (1 to 3), position (toe, intermediate and/or top), size and thickness of reams. The authors show that two reams are sufficient, one placed at the toe and the other positioned in the intermediate portion of the shaft with a spacing of three times the ream width, regardless of the ream thickness.

2. Objective

In this sense, the objective of this present study is to carry out a study to verify the influence of the under-reams on the load capacity of precast piles. For this, load tests were carried out in the laboratory, in scaled-down models, using optimized dimensions (double under-reamed: the width of the reams is twice as wide as the pile shaft and spacing between the reams three times the width). Additionally, other two configurations with one ream were tested. To understand the behaviour of the reams, especially in the load capacity, numerical simulations (finite element method) were carried out. The numerical was used to obtain (a) the load-settlement curves of the tests, (b) the concentration of plastic deformation zones in the soil, and (c) the normal and shear stresses that act along of the sides of the piles. From the numerical analysis it was possible to quantify the contribution of the reams in the total load capacity.

3. Description of laboratory load tests

The numerical study was based on compression load tests on scaled-down laboratory models, carried out in square section precast piles (mortar), with reduced dimensions, 50 cm long and 5 cm on the shaft side, making a 1:4 scale with a stake in true greatness. A pile without reams was used (as a reference test) and 3 under-reamed with 10 cm wide and 2.5 cm thick reams: (a) one at the toe (Ba), (b) two - toe and intermediate (BMa) and (c) an intermediary (Ma). The BMa pile (one ream at the toe and another intermediate) is the model that presents the optimized geometry (in preview parametric analysis). This arrangement maximizes the load capacity, because it has a distance of 30 cm between the reams (3 times the width of the ream) and minimizes the effects of one ream on the other (as verified by Christopher and Gopinath, 2015 and confirmed by Jong, 2019; Ruver et al., 2019).

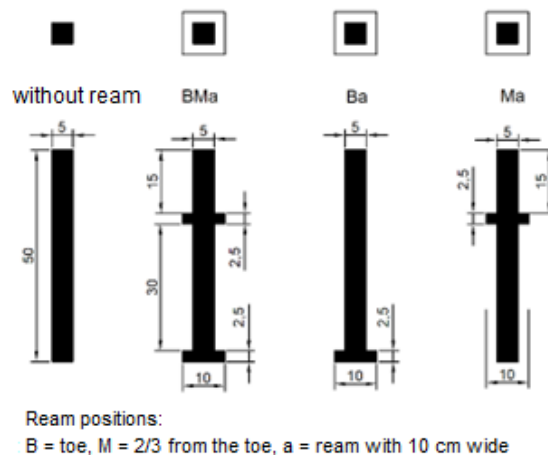The Fig. 1 shows the scaled-down piles with their dimensions.

Ream positions:
B = toe, M = 2/3 from the toe, a = ream with 10 cm wide

Figure 1. Dimensions of the scaled-down precast piles load tested in the laboratory.

The tests were carried out in a stainless tank with a diameter of 70 cm and a height of 70 cm. To carry out the tests, the tank was filled with fine aeolian sand, from Osório, Brazil ($\gamma_s = 2.65$ g/cm^3, $e_{min} = 0.6$ and $e_{max} = 0.9$). The sand was compacted in 10 cm layers with a manual wooden socket, in the wet state (average humidity of 20%) until obtaining a specific dry weight of (γ_d) = 1.56 g/cm^3 (equivalent to a density of 66.67% - medium condition). After compacting the sand and submersion with water, the piles were driven. Initially, two piles were driven without reams, one being driven by percussion (free fall hammer) and the other by pressing with a hydraulic jack, which served as a reference for load capacity. The other piles were driven by water jet with a flow rate of 2.5 m^3/h and a jet speed of 5.89 m/s (21.21 km/h) (due to the injector tube diameter of 12.5 mm), with the aid of a motor pump. At the end of the water jet setting, the excess water was drained off, leaving a thin film of water on the sand top layer.

The next step was to carry out the compression load tests. The applied loads were measured with an S-type load cell with a capacity of 20 kN. The displacements (settlements) were measured through two displacement transducers with a total stroke of 50 mm, installed in opposite positions. For the compression tests, the metallic structure of the laboratory and a hydraulic jack with a load capacity of 50 kN, manually operated, were used as a reaction system. As it is sand, method A, rapid test, of the ASTM D 1143M standard (ASTM, 2020) was adopted, which guides that the load test be performed by incremental load, with each increment of 5% of the probable breaking load, being maintained for a minimum time of 4 minutes and a maximum time of 15 minutes.

4. Description of numerical model

For numerical modelling, the finite element method (FEM) was used. A three-dimensional (3D) modelling was used, because of the square piles and a cylindrical tank. The dimensions of the sand inside the tank (a cylinder with 70 cm in diameter and 70 cm in height) and the piles (square bars with 5 cm of side and 45 cm in

length, although the total length was 50 cm) were the same used in the tests. For the fluidized zone, a prismatic region around the pile was considered, with a width equal to twice the largest width of shaft of the piles (as verified experimentally, regardless of the compactness of the sand, by Passini, 2015). For example, for the piles without reams, with 5 cm of side (uniform), a width of the fluidized zone of 10 cm was considered; for under-reamed piles (with 10 cm of side) a width of the fluidized zone of 20 cm was considered. For the bottom, a reach of 5 cm was considered, and this pattern was adopted for all piles driven by water jet. As for the boundary conditions, displacements in the three dimensions were prevented for the bottom (x = 0, y = 0, and z = 0); while on the sides only vertical displacements were allowed, preventing horizontal deformations (x = 0, y = 0, z = free), and the surface (top of the tank) was free.

For the material properties, as the piles were precast with mortar, an elastic constitutive model was assigned because the structural behaviour was not the focus of the present study, with an estimated modulus of elasticity compatible with the resistance of the mortar. While for the compacted (unfluidized) and fluidized sand, the perfectly plastic elastic model was adopted, with Mohr-Coulomb failure criterion, with the parameters of elasticity modulus and friction angle initially obtained from Corte et al. (2017), being adjusted by retro analysis. Table 1 shows the properties used in numerical modelling.

Table 1. Material properties used in numerical modelling

Material	ρ_{subm} (ton/m³)	E (MPa)	ν	ϕ' (°)	ψ (°)	c' (kPa)
Pile		20,000	0.2	-	-	-
Compacted sand	0.85	3.0	0.3	28	7.5	~2
Fluidized sand		1.8	0.3	20	0	~2

Where: ρ_{subm} is the submerged specific mass (for reasons of convergence, the same was adopted for all materials, in this case the value of compacted sand was adopted); E is the modulus of elasticity; ν is Poisson ratio; ϕ' is the effective friction angle, ψ is the dilation angle; c' is the cohesive intercept (even though it is zero for sand, but for software convergence reasons, a minimum and non-zero value must be assigned)

Numerical modelling was divided into two steps: (a) application of geostatic conditions (gravity acceleration equal to 10 m/s²) and (b) loading at the top of the piles (total vertical displacement of 50 mm, applied in 50 increments, i.e., 1 mm each increment). The displacement was applied to the top central node (master point), the entire top face being linked to this node (slave surface), so that each displacement applied results in a reaction load on the same node. As it is a drained condition, the load application time does not present interference and steps of 1 second are adopted. In the contact interfaces, two configurations were used: (a) rigid connection type (tie) (fluidized and unfluidized sand) and (b) friction interaction type (with a roughness of 0.3) and adhesion (hard contact) (sand and pile). The discretization of the mesh was made by rectangular elements of the structured type, with the central elements

formed with a spacing between the nodes of 25 mm. For the edge nodes, a spacing of 50 mm was adopted. As it is a three-dimensional modelling, elements composed of 8 nodes were used (corners, more in the central nodes), with reduced integration and processing time control. The average run time of each model was 3 hours. Fig. 2 shows examples of mesh discretization.
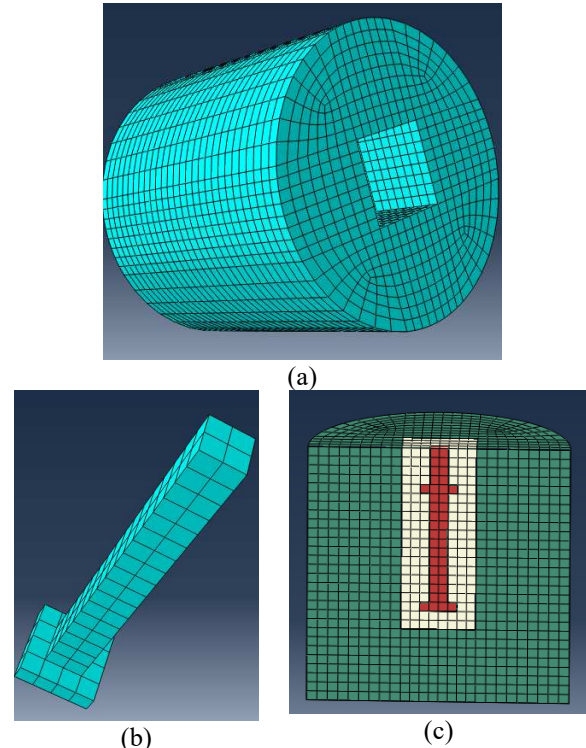

(a)

(b)

(c)

Figure 2. Examples of mesh discretization, being (a) from compacted sand (without fluidized sand and without pile), (b) from a pile and (c) view of the half of the 3D numerical model adopted for modelling the doble (toe and intermediate) under-reamed pile (BMa).

5. Results of Numerical Modelling

The Fig. 3 to Fig. 8 present the results of load-settlement obtained in the numerical modelling in comparison with the results of the laboratory load tests carried out with the scaled-down models. From the results it is possible to verify that up to a certain load level the numerical models converge with the test results, at least up to settlements of the order of 7.5 mm (15% of the pile side/diameter = 15% of 50 mm = 7.5 mm, which corresponds to the rupture criterion of the ASTM D 1143M standard). For large loads (and settlements) it is verified that some of the tested piles presented problems during the tests, such as ream breakage, which does not occur in numerical modelling, because an elastic model was used for the piles. In this way, it is possible to validate the numerical modelling, as well as to validate the properties attributed to the materials.

By analysing the results (specifically the Fig. 8), using the pile driven by percussion/pressing as a reference, it appears that the same pile (without ream driven with water jet), there is a reduction in the load capacity under compression, while the under-reamed

pile, recovers this load capacity, which is even higher, depending on the quantity and position of the reams. The performance of under-reamed piles with two reams (one at the toe and one in the intermediate position) is superior to the under-reamed pile with one ream (toe or intermediate position). For the under-reamed pile with one ream, it is observed that for small displacements, the pile with ream at the toe (Ba) has a greater stiffness, and for greater settlement, the pile with intermediate ream (Ma) presents better performance, being the same behaviour observed in laboratory tests.
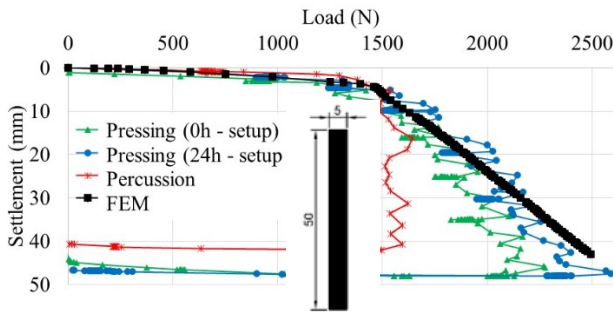

Figure 3. Comparison between numerical results and load tests (load - settlement) for pile without ream driven by percussion and pressing (pile dimensions in cm).
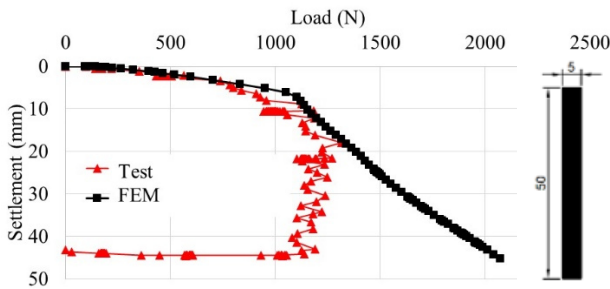

Figure 4. Comparison between numerical results and load tests (load - settlement) for pile without ream driven by water jet (pile dimensions in cm).
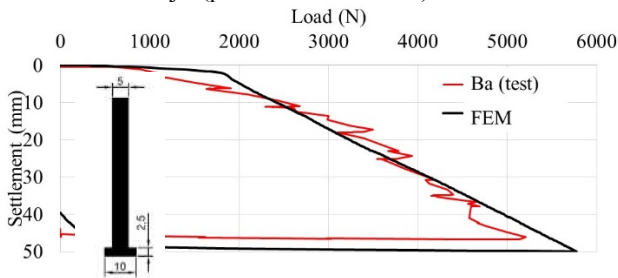

Figure 5. Comparison between numerical results and load tests (load - settlement) for toe under-reamed pile (Ba) by water jet (pile dimensions in cm).
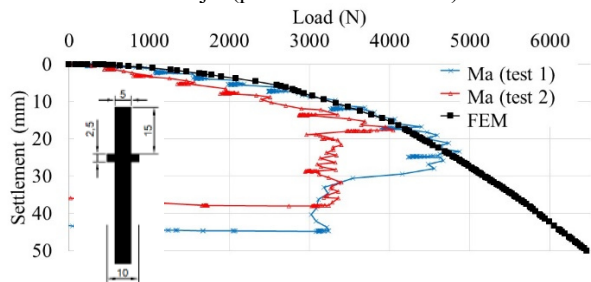

Figure 6. Comparison between numerical results and load tests (load - settlement) for intermediate under-reamed pile (Ma) by water jet (pile dimensions in cm).
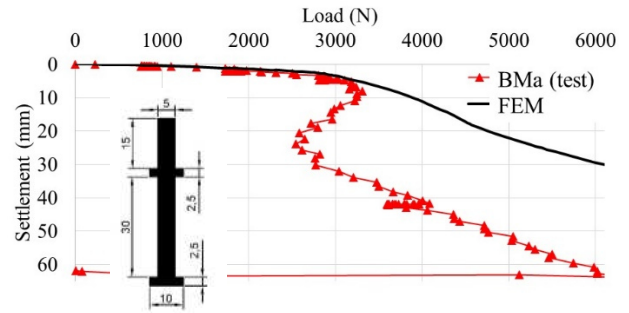

Figure 7. Comparison between numerical results and load tests (load - settlement) for doble (toe and intermediate) under-reamed pile (BMa) by water jet (pile dimensions in cm)
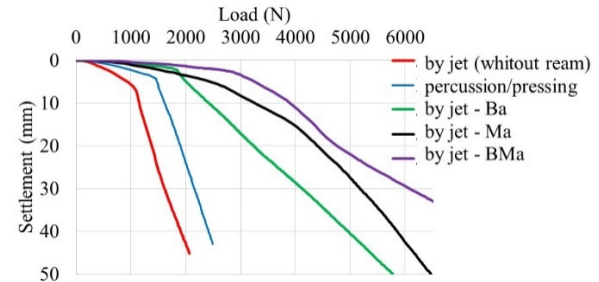

Figure 8. Numerical results of all load test (load-settlement)

To better understand the behaviour of the under-reamed piles, Fig. 9 to 11 show the plastic deformations for the 7.5 mm of settlement. For Fig. 9 the under-reamed pile with a ream at the toe (Ba), at small settlements, the plastic deformations are concentrated along the sides of the ream, reaching a larger area below and a smaller one above, concentrated inside the fluidized zone. For large deformations, the pattern is maintained, but with advancement of the plastic zone around the ream. For Fig. 10 the under-reamed pile with an intermediate ream (Ma), with small settlements, there are plastic deformations along the sides of the ream and toe, also reaching a region below and above the ream and toe, the lower one being larger, but within the zone fluidized, pattern maintained for large displacements (50 mm), but with plastic deformations they start to act along the entire shaft advancing to the surface. For the double under-reamed pile in Fig.11, at small deformations, the formation of a plastic zone occurs within the fluidized zone that covers the upper part of the intermediate ream, advances vertically in the perimeter of the ream reaching the lower base of the base ream. It is verified that the sand region between the reams do not undergo plastic deformation; with increasing pile displacement, an expansion of this zone occurs around the piles, but the region between the two reams are not affected by the plastic zone. In the case of the double under-reamed pile, it is possible to verify that the distance between the reams is 30 cm, which corresponds to a ratio of 3 times. In the literature, from this distance between the reams, it appears that they act individually, enhancing the load capacity. Also, for the double under-reamed (BMa) (Fig. 11), there is the formation of a plastic zone reaching all the fluidized sand and the toe considerably invades the unfluidized sand.
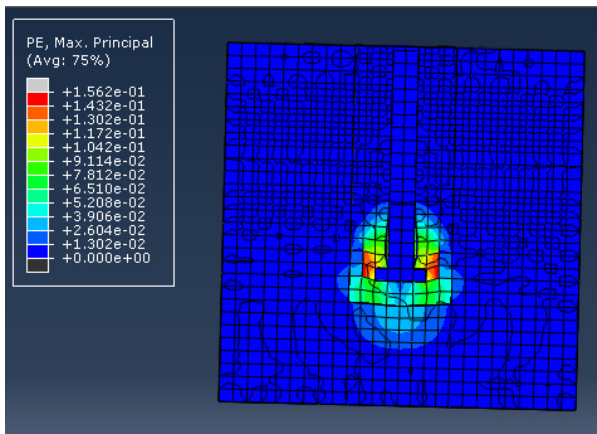
Figure 9. Plastic deformations at 15% (7.5 mm) of settlement for the toe under-reamed pile (Ba).
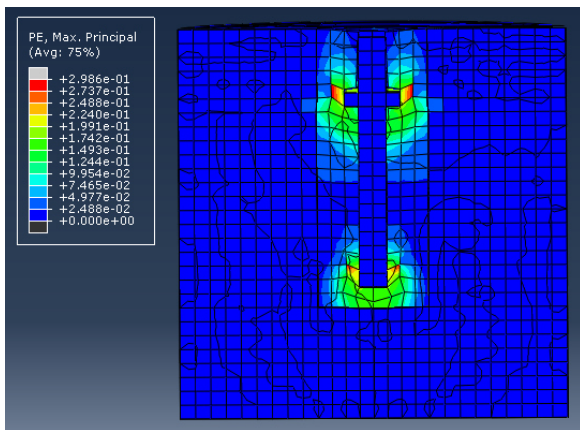

Figure 10. Plastic deformations at 15% (7.5 mm) of settlement for the intermediate under-reamed (Ma).
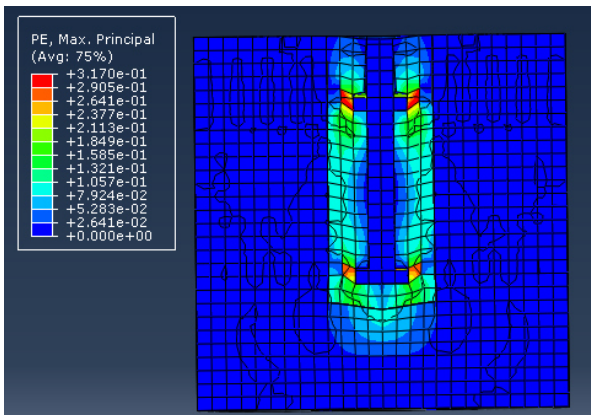

Figure 11. Plastic deformations at 15% (7.5 mm) of settlement for the doble (toe and intermediate) under-reamed pile (BMa).

Another information that can be obtained by numerical modelling is the quantification of the contribution of each of the components in the total load capacity. In the case of uniform piles (without reams), the load capacity is composed of lateral friction and toe load (compression). In the case of under-reamed piles, in addition, there is the contribution of reams, which generate compression loads in the soil. In this case, to obtain the toe and ream loads, the distribution of compressive stresses under bottom the faces is obtained and integrated by the area. For lateral friction, obtain the distribution of shear stresses along the length of the shaft and side of the reams, integrating the lateral area. Table 2

(in load - kN) e 3 (in percent of load capacity) present a compilation of the contribution of each of the parts in the total load capacity, for a settlement of 7.5 mm.

Table 2. Contribution (in kN) of the load capacity of each element of the piles for a settling level of 7.5 mm

Load / Pile:	P/P	J	Ba	Ma	BMa
Toe	1.514	1.077	0.936	1.220	1.720
Toe ream	-	-	1.265	-	0.920
Intermediate ream	-	-	-	1.641	0.760
Lateral Friction	0.062	0.050	0.005	0.001	0.190
Total (kN)	1.576	1.127	2.206	2.862	3.590

Where: P/P = average value by percussion and pressing driven; J = jet water driven of pile without under-ream; Ba, Ma and BMa specified in Fig. 1 driving by jet water

Table 3. Contribution (in percent) of the load capacity of each element of the piles for a settling level of 7.5 mm

% / Pile:	P/P	J	Ba	Ma	BMa
Toe	96.1	95.6	42.4	42.6	47.9
Toe ream	-	-	57.3	-	25.6
Intermediate ream	-	-	-	57.3	21.2
Lateral Friction	3.9	4.4	0.2	0.03	5.3

In the analysis of the piles without ream, it appears that the piles driven by conventional techniques (percussion and pressing) presented a total average load capacity of 1.576 kN, while the pile driven by water jet presented a total load capacity of 1.127 kN, which corresponds to a reduction of 28.5%. But it is possible to notice that both have the same distribution of the portion referring to the toe and lateral friction, and almost all the contribution is due to the toe (more than 95%).

The under-reamed pile with a ream at the toe (Ba model) had a total load capacity of 2.206 kN, a value 40% higher than that of conventional driving and twice that of the pile without ream driven by water jet. For this pile, the toe load corresponds to almost the entire load capacity (99.7%), with the contribution due to the increase in the area referring to the ream of 57.3% (which is greater than the toe contribution - 42.4%). This occurs because the ream prevents the lateral friction mobilization of the shaft above it, and it was found that lateral friction mobilization occurred along the sides of the ream and in an area near the top of the pile. Along the rest of the shaft there was no mobilization of lateral friction.

For the under-reamed pile with an intermediate ream (Ma model) there is a total load capacity of 2.862 kN, which is 82% higher compared to conventional piles. In addition, the intermediate ream proved to be more efficient than the toe ream. In terms of the contribution of the ream, there was a contribution of 57.3% of the ream in the load capacity, while the toe shows a contribution of 42.6%. Similar to the toe-reamed case, the contribution portion of the shaft was very low, for the pile with an intermediate ream, almost insignificant, at 0.03% of the load. In this case, it was found that there was only mobilization of lateral friction along the lateral faces of the reams. In the case of under-reamed piles with

one ream (Ba and Ma), the toe capacity is like the toe capacity of the pile without ream driven by water jet, which shows that the significant increase in the load capacity of the under-reamed piles is due to the reams (57.3%).

The under-reamed pile with two reams (BMa) presented superior performance to the others, 3.59 kN of load, which corresponds to more than double (127.8%) in relation to the reference pile and more than triple that of the pile without ream driven by water jet. In terms of the contribution of the reams, both presented similar contributions of 21.2% and 25.6%, intermediate and toe (portion referring to the increase in area), respectively, corresponding together about half of the load capacity. These values show that these dimensions enhance the load capacity, conforming to the parametric numerical modelling previously carried out by Jung (2019) and Ruver et al. (2019).

6. Conclusions

Through the present study, it was possible to verify that the use of under-reamed precast piles, not only recover the total load capacity lost by the harmful effect of the water jet, but also present a higher total load capacity than to a pile section uniformly driven by percussion (or pressing), reaching values that double for the optimized geometry model, with two reams, the ream width being twice the width of the pile side, as well as a spacing between the ream of three times the ream width.

Numerical modelling proved to be efficient as it was able to reproduce the load-settlement curves obtained in the load tests with the reduced models. In addition, it was possible to obtain the diagrams of plastic deformation of the soil and the normal and shear stresses that act along all the pile faces. These elements were of fundamental importance, as they allowed us to understand the behaviour of the reams, as well as made it possible to estimate the load contribution of the reams to the total load capacity of the piles.

Acknowledgements

References

Brazilian Association of Technical Standards (ABNT) (English translation). "NBR 6122: Design and Execution of Foundations". Rio de Janeiro, Brazil,2019, 108 p. (in Portuguese).

American Society for Testing and Materials (ASTM). "D 1143: Standard test methods for deep foundation elements under static axial compressive load". Philadelphia, PA, USA, 2019, 15 p.

Choi, Y.; Kim, D-C.; Kim, S-K.; Nam, M S.; Kim, T-H. "Implementation of noise-free and vibration-free PHC screw piles on the basis of full-scale tests". American Society of Civil Engineers, ASCE, Journal of Construction Engineering and Management, 139(8), 2013, pp 960-967. http://dx.doi.org/10.1061/(ASCE)CO.1943-7862.0000667

Christopher, T., Gopinath. B. "Parametric study of under-reamed piles in sand". International Journal of Engineering Research & Technology (IJERT), v. 5 (7), 2016, pp 577-581. (Available at: https://www.ijert.org/research/parametric-study-of-under-reamed-piles-in-sand-IJERTV5IS070450.pdf, 29/09/2022).

Corte, M. B.; Festugato, L.; Consoli, N. C. "Development of a Cyclic Simple Shear Apparatus". Soils and Rocks, 40(3), pp 279-289, 2017. (Available at: http://www.soilsandrocks.com.br/soils-androcks/SR40-3_279-289.pdf, 29/09/2022)

Das, B.; Sivakugan, N. "Principles of Foundation Engineering". 9th edition, Cengage Learning: Sandford, USA, 2018, 994 p.

George, B. E.; Hari, G. "Numerical investigation of under-reamed pile". In: The Sixth International Geotechnical Symposium" Chennai, India, 2015, 4p. (Available at: http://www.igs.org.in:8080/portal/igc-proceedings/igc-2016-chennai-proceedings/theme2/IGC_2016_paper_487.pdf, 29/09/2022).

Gunaratne, M.; Hameed, R.A., Kuo, C., Reddy, D.V., Patchu, S. "Investigation of the effects of pile jetting and preforming". Thechnical Repport N. 772, Florida Department of Transportation, 2019, 137 p.

Hirai, Y., Wakai, S., Aoki, M. "Development of multi-belled cast-in-place concrete pile construction method" AIJ. Journal of Technology and Design. v. 14, nº 28, 2018, pp 433-438. https://doi.org/10.3130/aijt.14.433

Honda, T.; Hirai, Y.; Sato, E. "Uplift capacity on balled and multi-belled piles in dense sand". Japanese Geotechnical Society. Soil and Foundations, v. 51, nº 3, 2011, pp 483-496. https://doi.org/10.3208/sandf.51.483

Jong, G.V.D "Numerical modeling of the behavior of ribbed piles driven by water jet", (English translation). Graduation work. Federal University of Rio Grande do Sul, Brazil, 2019, 108 p. (in Portuguese) [online] Available at: http://hdl.handle.net/10183/200223, 29/09/2022.

Lee, C.Y. "Settlement and load distribution analysis of underreamed piles". ARPN. Journal of Engineering and Applied Sciences, v. 2, nº 4, 2017, pp 36-40. (Available at: https://citeseerx.ist.psu.edu/viewdoc/download?doi=10.1.1.565.1016&rep=rep1&type=pdf, 29/09/2022)

Majumder, M., Chakraborty, D. "Bearing capacity of under-reamed piles in clay using lower bound finite element limit analysis". International Journal of Geotechnical Engineering, 16:9, 2022, pp. 1104-1115. https://doi.org/10.1080/19386362.2022.2044102

Mezzomo, S.M. (2009). "Study of sand fluidization mechanisms with water jet", (English translation). Msc. Dissertation. Federal University of Rio Grande do Sul, Brazil, 2019, 230 p. (in Portuguese) [online] Available at: http://hdl.handle.net/10183/23970, 29/09/2022

Moayedi, H., Mosallanezhad, M. "Uplift resistance of belled and multi-belled piles in loose sand". Measurement. Elsevier, 190, 2017, pp 346–353. https://doi.org/10.1016/j.measurement.2017.06.001

Mohan, D., Murthy, V.N.S., Jain, G.S. "Design and construction of multi-underreamed piles". In: 7th International Conference of Soil Mechanics and Foundation Engineering. Mexico City, Mexico, v. 2, 1969, 183-186.

Moriyasu, S., Ishihama, Y., Takeno, T., Taenaka, S., Kubota, K., Tanaka, R.; Nishiumi, K., Harata, N. "Development of new-type steel-pile method for port facilities". Nippon Steel & Sumitomo Metal Technical Report. N. 113, 2016a, pp 49-56. (Available at:

https://www.nipponsteel.com/en/tech/report/nssmc/pdf/113-07.pdf, 29/09/2022).

Moriyasu, S., Morikawa, Y., Yamashita, H., Taenaka, S. (2016b). "Evaluation of the vertical bearing capacity of steel pipe piles driven by the vibratory hammer Method with water and cement milk jetting". In: The 15th Asian Regional Conference on Soil Mechanics and Geotechnical Engineering. Japanese Geotechnical Society Special Publication, 2016b, pp 1291-1295. https://doi.org/10.3208/jgssp.JPN-126

Passini, L.B. "Installation and axial load capacity of fluidized model piles in sandy soils", (English translation). Dsc. Theses. Federal University of Rio Grande do Sul, Brazil. 2015, 275 p. (in Portuguese) [online] Available at: http://hdl.handle.net/10183/131011, 29/09/2022.

Ruver, C.A. "Study of the behavior of precast piles driven by water jet", (English translation). Internal Research project report. Federal University of Rio Grande, Brazil, 2013, 108p. (in Portuguese).

Ruver, C.A., Ferronato, B., Dalla Vecchia, D., Spaniol, E.M.R., da Silva, G.G., Palomino, J. M.V. (2014). "Comparison between percussion and water jet driving", (English translation). In: XVII COBRAMSEG - Brazilian congress of soil mechanics and geotechnical engineering, Goiania, Brazil/GO; 2014, pp. 1-10. (in Portuguese).

Ruver, C.A, Jong, G.V.D. "Water jet driven under-reamed piles: parametric analysis of the influence of compactness", (English translation). In: GeoRS - Geotechnical Engineering Seminar of Rio Grande do Sul, Santa Maria, Brazil, 2019, pp. 1-9. (in Portuguese) (Available at: http://www.bibliotecadigital.ufrgs.br/da.php?nrb=001097518&loc=2019, 29/09/2022).

Ruver, C.A., Jong, G.V.D, Peres, M. S. "Numerical modelling of the behaviour of ribbed piles driven by water jet", (English translation). In: XII GEOSUL - Southern Region Geotechnical Engineering Practices Symposium, Joinville, Brazil, 2019, pp. 1-10p. (in Portuguese) (Available at:

https://conferencias.ufsc.br/index.php/geosul2019/2019geosul/paper/view/363/448, 29/09/2022).

Shetty, P., Naveen, B.S., Naveen, K.B.S. "Analytical study on geometrical features of under-reamed pile by ansys". International Journal of Modern Chemistry and Applied Science, 2 (3), 2015, pp. 174-180.

Tsinker, G. "Pile jetting". American Society of Civil Engineers, ASCE, Journal of Geotechnical Engineering, 114(3), 1988, pp. 326-334.

Vali, R., Khotbehsara, E M.; Saberian, M., Li, J.; Mehrinejad, M., Jahandari, S. "A three-dimensional numerical comparison of bearing capacity and settlement of tapered and under-reamed piles". International Journal of Geotechnical Engineering. Taylor & Francis Group, 13:3, 2017, pp. 236-248. https://doi.org/10.1080/19386362.2017.1336586

Yabuuchi, S., Hirayama, H. "Bearing mechanisms of nodal piles in sand. Deep foundations on bored and auger piles". Balkema, Rotterdam. 1993, pp. 333–336. (Available at: http://www.japanpile.co.jp/ir/uploads/09_36.pdf, 29/09/2022).

Zarrabi, M.; Esmali, A. "Behavior of piles under different installation effects by physical modeling". American Society of Civil Engineers, ASCE, International Journal of Geomechanics, 16 (5), 2016, pp. 1532-3641. http://dx.doi.org/10.1061/(ASCE)GM.1943-5622.0000643

Zhang, L., Chen, Q., Gao, G., Ninbalkar, S., Chiaro, G. "A new failure load criterion for large-Diameter under-reamed piles: practical perspective" International Journal of Geosynthetics and Ground Engineering. 4:3, 2019, pp. 1-9. http://dx.doi.org/10.1007%2Fs40891-017-0120-8

Ziyara, H. M., Albusoda, B. S. "Experimental and numerical study of the bulb's location effect on the behavior of under-reamed pile in expansive soil". Journal of the Mechanical Behavior of Materials, v. 31, n°. 1, 2022, pp. 90-97. https://doi.org/10.1515/jmbm-2022-0010